Synthesis of Zeolite Y from Kaolin and Its Model Fuel Desulfurization Performance: Optimized by Box-Behnken Method

Honarmand, Somayyeh
Chemical Engineering Department, Tarbiat Modares University, Tehran, I.R. IRAN

Mousavi, Elham Sadat
Chemical and Materials Engineering, Buein Zahra Technical University, Buein Zahra, Qazvin, I.R. IRAN

Karimzadeh, Ramin*+
Chemical Engineering Department, Tarbiat Modares University, Tehran, I.R. IRAN

ABSTRACT: *In this research, zeolite Na-Y was synthesized from Kaolin without an organic template under the non-hydrothermal condition to adsorb sulfur compound. Model fuel desulfurization was optimized by employing the Box-Behnken experimental design with 2 center points, the three parameters, and one response value. The objective was to find how sorption capacity is related to alkali fusion temperature, crystallization time, and aging time. Optimal DBT adsorbent was synthesized at 550 °C, minimum crystallization time, and maximum aging time. The zeolite samples were characterized by FT-IR and XRD. The crystallinity of the samples was lower than the crystallinity of commercial zeolite Y. During zeolite preparation, there was a competition between zeolite Na-Y, Na-P, Na-X and Na-A. The equilibrium results were well fitted by the Langmuir and Freundlich isotherms for the best adsorbent. The largest DBT adsorption capacity, 32.67 mg DBT/g, was calculated for the optimal adsorbent. Pseudo-first order and pseudo-second-order models were evaluated to understand the kinetics of the adsorption process. The reduction of DBT obeyed the second-order model of kinetic. Ni-Y and La-Y zeolites were prepared by the liquid-phase ion-exchange method. The maximum DBT adsorption capacity has been observed for Ni–Y (~ 72.25 mg DBT/g) and La–Y (~ 66.59 mg DBT/g).*

KEYWORDS: *Zeolite Y; Kaolin; Dibenzothiophene; Langmuir isotherm; Adsorption kinetic*

INTRODUCTION

The **p**resence of Sulfur causes environmental pollution. Upon combustion in car engines, the organic sulfur compounds of the fuel convert to SO_x products. It may cause acid rains, as well as a high content of sulfuric oxides in exhaust fumes decreasing the yield of catalytic converters in vehicles. As a result, CO and NO_x emission

** To whom correspondence should be addressed.*
+ E-mail: ramin@modares.ac.ir
1021-9986/2020/1/79-90 12$/6.02

contents would increase causing growing negative environmental effects [1, 2]. There are new rules, enacted and promoted by different organization all over the world, e.g. EPA in the USA, that force refineries to cut sulfur levels of gasoline to 30 ppm and for diesel up to 15 ppm, by 2006 [3, 4]. Well known desulfurization methods mostly include Catalytic Cracking Desulfurization, Hydrodesulphurization, Ultra-sonic Desulfurization, Adsorption Desulfurization, Organic Solvent Extraction Desulfurization, Biodesulfurization, Ionic Liquid Desulfurization and Oxidation Desulfurization. To study all of desulfurization methods, Adsorption Desulfurization can selectively eliminate sulfide in petroleum fuels under room temperature without hydrogen, which is contemplated as a very effective and economic technique. The basic principle of Adsorption Desulfurization is to utilize solid adsorbent to selectively adsorb sulfur compounds in petroleum fuels. Reduction of dibenzothiophene from model fuel was performed by adsorption on commercially available adsorbents, including an activated carbon, aluminum oxide, A, 13X, and Y zeolite[5, 6]. Having a 3-dimensional porous structure similar to LTA, Zeolite Y also exhibits FAU (faujasite) structural characteristics while being made of secondary building units 4, 6, and 6-6. The framework of Zeolite Y consists of β-cage (sodalite) and α-cage (super cage). *β*-cages are linked together by double six membered rings (D6R). The pore diameter is large at 7.4 Å since the aperture is defined by a 12 members oxygen ring leading into a larger cavity of diameter 12Å. The cavity is surrounded by ten sodalite cages (truncated octahedral) connected to their hexagonal faces. The unit cell is cubic (a= 24.7Å) with Fd-3m symmetry. Zeolite Y has a void volume fraction of 0.48, with different framework Si/Al ratios between 1.5< Si/Al<3[7, 8]. Yang used Cu^{I}/Y and Ag^{I}/Y to adsorb sulfur compounds from commercial fuels at ambient temperature and pressure and reported that the sulfur content was reduced from 430 to <0.2 ppm by weight with a sorbent capacity of 34 cm^3 of clean diesel produced per gram of sorbent[9]. Velu, Ma, and Song reported that Ce-exchanged Y zeolites exhibited excellent adsorption capacity[10]. *Yang et al.* reported that Ag^{+}, Cu^{+}, Ni^{2+}, and Zn^{2+} ion-exchanged Y zeolite adsorbents represented high sulfur adsorption capacity for thiophenic compounds. Among all the ion-exchanged Y zeolites, $Cu^{I}Y$ showed the highest sulfur adsorption capacity, at the same test conditions[11, 12] . Zhitao et al reported that LaY zeolite achieved the best desulfurization effect at an adsorption temperature of 45 ℃ and an adsorbent/oil ratio of 1:2[12].

In this research, we study non-hydrothermal transformation of kaolin into zeolite Na-Y. During preparation of zeolite Y from kaolin, the effect of various parameters such as ageing time, crystallization time, and alkali fusion temperature, on the adsorbents were investigated. Desulfurization of fuel model was carried out in a batch system and the process was optimized by using Response Surface Methodology (RSM). The Ni-Y and La-Y zeolites were prepared by liquid-phase ion-exchange method. Model fuel desulfurization by Ni-Y and La-Y was studied, as well.

EXPERIENTAL SECTION

Preparation of Zeolite Y from Kaolin

Conventional materials were used as starting materials. In order to prepare zeolite Y from kaolin, kaolin was fused with NaOH (Kaolin /NaOH =1/1.5 in weight) at 750°C for 3h. After fusion, the fused kaolin was cooled and grounded. Ten grams of fused kaolin powder and 12.68 grams of sodium silicate were dissolved in 150 ml of deionized water followed by stirring for 1h at room temperature. The mixture was aged for 1 day at room temperature. Then, the mixture was refluxed for 12h at 100°C. Subsequently, the zeolite product was filtered, washed with deionized water, and dried [13-25].

Adsorption Experiment

Adsorption of DBT was carried out in a stirred batch system at room temperature. By adding 0.1g of adsorbent to 10 mL n- hexane solutions of DBT, we then stirred the mixture at room temperature. The equilibration time was chosen based on kinetic studies. The adsorbent was separated from the liquid phase by filtration. Concentrations of equilibrated solutions were determined by UV spectroscopy instrument (Optizen 3220 UV) at a wavelength of 325 nm. The amount of adsorbed DBT was calculated by the following equation:

$$q_e = V(C0 - Ce)/m \quad (1)$$

Where, q_e is the adsorbed amount (mg DBT/g adsorbent), V is the volume of solution (L), m is the mass

Table 1: Actual and coded values of factors [13].

Factor	Unit	Low level	Center level	High level
(A): alkali fusion temperature	°C	550	650	750
(B): crystallization time	h	12	18	24
(C): aging time	h	16	24	32

of adsorbent (g) , while C0 and Ce are initial and equilibrium concentrations (mg DBT /L), respectively [26, 27].

Response Surface Methodology

Response Surface Methodology (RSM) employs the mathematical and the statistical approaches for developing, improving, and optimizing processes. It was applied here for design and analysis of experiments to describe relation of sorption capacity (q) to the three synthesis parameters of zeolite Y: alkali fusion temperature, crystallization time, and aging time. Model fuel desulfurization was optimized by applying Box-Behnken experimental design with 2 center points (Table 1). We used three parameters: alkali fusion temperature (A: T, °C), crystallization time (B: cris, hour), and aging time (C: aging, hour). BBD is an efficient type of design with three levels for fitting second-order response surfaces [28, 29].

Model parameters were estimated using the following second order model:

$$Y = \beta + \sum_{i=1}^{k} \beta_i X_i + \sum_{i=1}^{k} \sum_{ij}^{k} \beta_{ij} X_i X_j \qquad (2)$$

Where, Y is the predicted response which represents sorption capacity (q) and output sulfur concentration (C_e); Xi and Xj are coded factors; β, βi, and βij are the model parameters, and k is the number of factors under study.

Modification of Prepared Zeolite Y

The Ni-Y and La-Y were prepared by liquid-phase ion-exchange method. Four grams of Y-zeolite was mixed with 80mL of 0.2 M aqueous solution of Ni $(NO_3)_2.6H_2O$ or La $(NO_3)_3.6H_2O$. Next the aqueous solutions were stirred for 24 h and at room temperature then filtered. After that the ion-exchanged samples were washed with deionized water, finally dried at 110°C for 24 h and calcined in air at 550°C for 4 h[30].

Characterization

The crystal structure was calculated by a Phillips XRD instrument with Cu Kα radiation (40 kV, 30 mA) and λ=1.540598 Å. A step size of 0.02 was used from a 2Θ angle of 5–80°. Crystalline phases were identified by comparison the reference data from the International Center for Diffraction Data (ICDD) database. Zeolite Y samples were determined utilizing a PerkinElmer spectrophotometer version (10.03.06) using KBr pressed disk technique. Spectrum was recorded in the wave range from 400 to 4000 cm^{-1} by step 1 cm^{-1}.

Kinetic Study

In order to gain a better understanding of adsorption process, the kinetic models are used to test experimental data. Adsorption kinetic was investigated by applying pseudo-first order and pseudo-second order models.

The pseudo-first order model is:

$$\ln(q_e - q) = \ln(q_e) - k_1 t \qquad (3)$$

Where, k_1 (min^{-1}) is the rate constant of the pseudo-first order adsorption, q (mg/g) is the amount of adsorbed DBT on the adsorbent at time t (min), and q_e (mg/g) is the equilibrium sorption uptake[22].

The pseudo-second order model is:

$$\frac{t}{q} = \frac{1}{k_2 q_e^2} + \frac{t}{q_e} \qquad (4)$$

Where, k_2 (g/mg.min) is the rate constant of pseudo-second order adsorption[31].

Adsorption Isotherms

Solutions of DBT were prepared with different concentrations. Equilibrium characterization of the adsorptive desulfurization was carried out by fitting experimental data to Langmuir and Freundlich isotherms. The equilibrium phrase of the Langmuir model is:

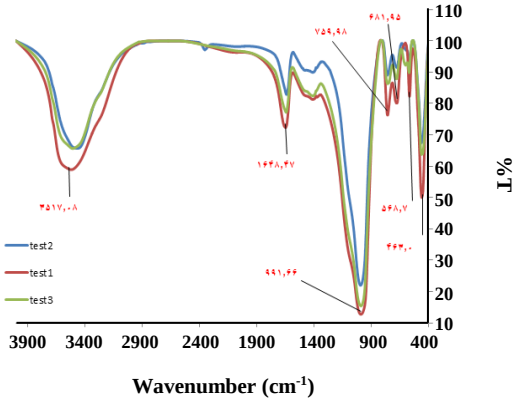

Fig. 1: FT-IR spectra of NaY (test1, test2 and test 3).

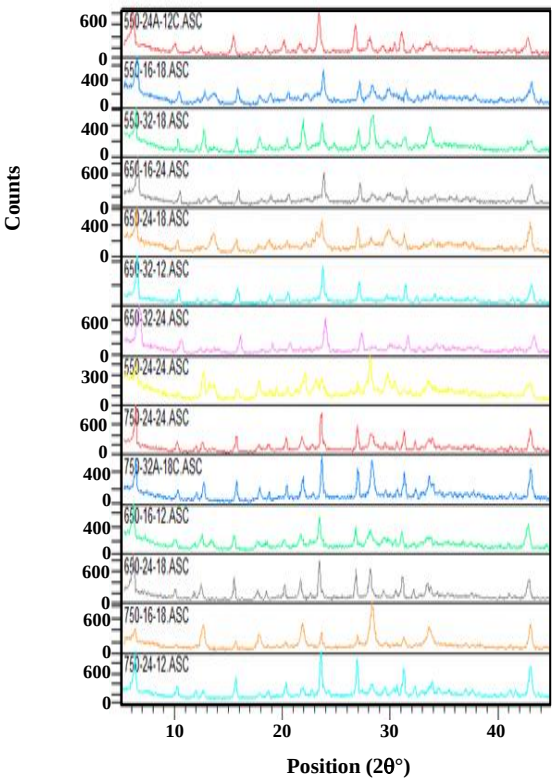

Fig. 2: XRD Pattern of zeolite Y.

$$q = q_m \frac{bc_e}{1 + bc_e} \quad (5)$$

Where, q_m is the maximum adsorption capacity (mg/g) under these working conditions, q is the amount of DBT adsorbed at equilibrium (mg/g), Ce is the equilibrium DBT concentration in solution (mg/L), and b is the constant of Langmuir adsorption equilibrium (L/mg). Maximum sorption capacity (qm) expresses monolayer envelopment of adsorbent and b represents affinity between the adsorbent and the sorbate.

In addition, the equilibrium parameter, R_L, was computed using the following phrase:

$$R_L = \frac{1}{1 + bC_0} \quad (6)$$

RL value indicates that the adsorption nature is either unfavorable if R_L>1, linear if R_L =1, favorable if 0< R_L<1, or irreversible if R_L=0.

The Freundlich isotherm is widely used to illustrate the adsorption features on the heterogeneous surface and takes the following form:

$$q = k_f \times C_e^{(1/n)} \quad (7)$$

Where k_f and n are equilibrium constants that are representative of adsorption capacity and adsorption intensity, respectively [31-35].

RESULTS AND DISCUSSION

Fourier Transmission Infrared Spectroscopy

FTIR spectrum is shown in Fig. 1 for zeolite NaY (alkali fusion temperature =750 °C, aging time= 24, crystallization time 12). Peak positions are nearly identical for the three samples. The peak at 463.02 cm^{-1} is assigned to the structure insensitive internal TO_4 (T=Si or Al) tetrahedral banding peak of zeolite Y. The peak at 568.71 cm^{-1} is attributed to the double ring external linkage peak defined to zeolite Y. The peaks at 759.98 and 681.95 cm^{-1} are assigned to external linkage symmetrical stretching and internal tetrahedral symmetrical stretching respectively. Furthermore, the peak at 991.66 cm^{-1} is assigned to internal tetrahedral asymmetrical stretching and peaks around 1648.47 and 3517.08 cm^{-1} are assigned to H-O-H banding and hydroxyl groups of zeolite, respectively[36-38].

X-Ray Diffraction

Formation of NaY zeolite in the fourteen samples, as the major peaks of identification on XRD pattern, were located at 2θ = 6.3, 10.2, 11.9 15.65, 18.7, 20.35, 23.6, and 26.95 (Fig. 2). Crystallinity of the synthesized zeolite Y was lower than crystallinity of the commercial zeolite Y. During the zeolite preparation, there are competition between zeolite Na-Y, Na-P, Na-X and Na-A (Table 2).

Table 2: Effects of the three synthesis parameters on Zeolite Formation.

alkali fusion temperature (A)	aging time (C)	crystallization time (B)	Product
550	16	18	X,Y
550	32	18	X,Y
650	16	24	X,Y
650	24	18	X,Y
650	32	12	X,Y
550	32	24	X,Y,A
650	16	12	P,Y
650	24	18	P,Y
750	16	18	P,Y
550	24	24	X,Y
750	24	24	X,Y,P
750	32	18	X,Y
750	24	12	P,Y
550	24	12	Y

Table 3: Desulfurization experiments plan and obtained results.

Run	A(ºC)	B(h)	C(h)	q(mg DBT/g)
1	550.00	18.00	16.00	16.81
2	750.00	18.00	16.00	17.13
3	750.00	24.00	24.00	18.97
4	750.00	12.00	24.00	20.56
5	750.00	18.00	32.00	24.69
6	550.00	12.00	24.00	19.36
7	650.00	12.00	16.00	15.35
8	650.00	18.00	24.00	15.35
9	650.00	24.00	16.00	11.77
10	650.00	24.00	32.00	21.3
11	650.00	18.00	24.00	12.44
12	550.00	24.00	24.00	15.15
13	650.00	12.00	32.00	22.77
14	550.00	18.00	32.00	26.15

Table 4: The analysis of variance (ANOVA).

source	sum of squares	df	Mean Square	F value	P-value	
model	235.99	8	29.5	14.99	0.0042	significant
A-T	1.88	1	1.88	0.96	0.3731	
B-CRIS	14.72	1	14.72	7.48	0.0411	
C-AGING	143.23	1	143.23	72.78	0.0004	
AB	1.72	1	1.72	0.87	0.3933	
BC	1.11	1	1.11	0.57	0.4859	
A^2	51.36	1	51.36	26.10	0.0037	
B^2	1.19	1	1.19	0.60	0.4727	
C^2	34.72	1	34.72	17.64	0.0085	
Residual	9.84	5	1.97			
Lack of Fit	5.61	4	1.40	0.33	0.8428	not significant
Pure Error	4.23	1	4.23			
Core total	245.83	13				

Table 5: The optimum values of variables.

	A	B	C
Range	550-750	12-24	16-32
Optimum value	550.25≈550	13.71≈12	31.95≈32

Response Surface Methodology

In this research, 14 synthesized zeolites were used for a three-factor design to satisfy Response Surface Methodology (Table 3). To identify the significance of the factors, their optimal values and interactions, also to obtain the best possible regression model for sorption capacity according to these factors, the experiments' results were statistically analyzed using Design-Expert© software. In these models, factor A is alkali fusion temperature, factor B is crystallization time, factor C is aging time, and AB and BC are interaction of the main parameters. The overall second-order polynomial equations for sorption capacity and output sulfur concentration in coded form were obtained as follows:

$$q_e = 13.90 + 0.48\times A - 1.36\times B + 4.23\times C + 0.66\times A\times B + 0.53\times B\times C + 4.01\times A^2 + 0.61\times B^2 + 3.29\times C^2 \quad (8)$$

The analysis of variance (ANOVA) was carried out (Table 4) and the results were used for validating the models and its coefficients. Optimum values of variables predicted by the model (aimed at maximizing sorption capacity) are presented in Table 5.

Fig. 3 shows the predicted response values calculated by the statistical model versus the actual response values obtained from the experiments. It confirms the suitability of the model since all points are located around the diagonal line.

Accumulation of the points around 45^0 indicates a satisfactory correlation between the experimental data and the predicted values which means the models is appropriate for response prediction.

Fig. 4 shows the second-order contour plot for adsorption capacity which depends on crystallization time and aging time when alkali fusion temperature was at fixed value of 550 (°C). As presented in Fig. 4, adsorption capacity decreases with increasing crystallization time with a constant aging time. Under constant crystallization time, an increase in adsorption capacity was observed for higher aging time. The highest adsorption capacity corresponded to the lowest value of crystallization time (12h) and the highest value of aging time (32h).

As it can be seen as it is shown in Fig. 5, center of the circle is the best condition to obtain the minimum adsorption capacity. The highest adsorption capacity corresponded to the lowest, the highest value of alkali fusion temperature and the lowest value of crystallization time (12h).

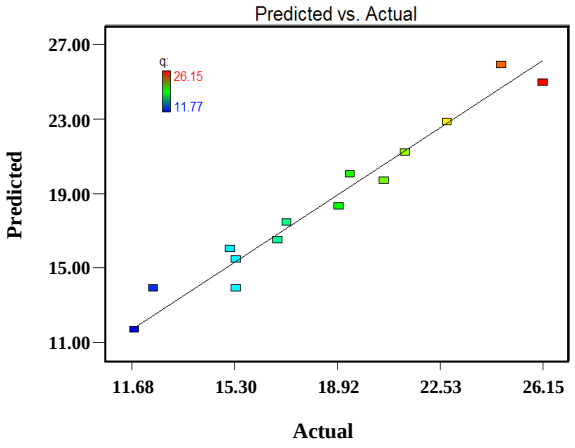

Fig. 3: Predicted vs. actual values of adsorption capacity.

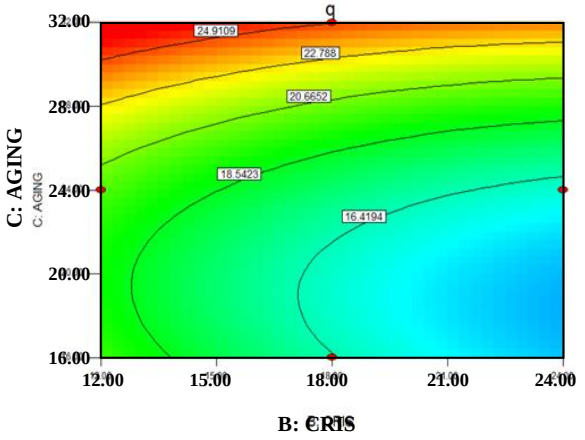

Fig. 4: Interaction effect of aging time(C) and crystallization time (B) on the adsorption capacity.

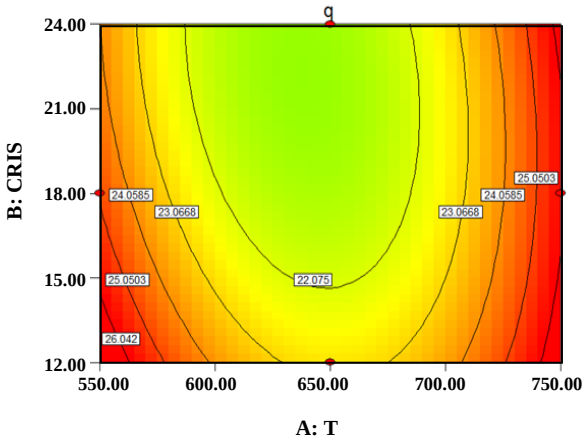

Fig. 5: Interaction effect of alkali fusion temperature (A) and crystallization time (B) on the adsorption capacity.

Kinetic Analysis

The effect of contact time on DBT adsorption by Na-Y zeolite at room temperature is shown in Fig. 6. Equilibrium state is achieved after 120 min. The obtained adsorption capacity was 14 mg DBT/g. Adsorption kinetic was investigated by applying pseudo-first order and pseudo-second order models. The results of kinetic analysis are presented in Figs. 7 and 8. Table 6 presents the results and correlation coefficients of the pseudo-first and pseudo-second order adsorption kinetic models.

This result along with the fact that the points on graphic interpretation of pseudo-second order model lie on the straight line and the correlation coefficient, R^2 value, is close to 1 suggest that kinetic of adsorption of DBT on Na-Y zeolite is described properly by the pseudo- second order model. Actually, it could also be explained by the value of $q_{e,cal}$ (15.015 mg/g, pseudo-second order model) which is more consistent with the adsorption capacity of 14 mg DBT/g in Fig. 6.

Adsorption Equilibrium Analysis

The values of equilibrium parameter, R_L, presented in Table 7, were all less than 1 and larger than 0; i.e. appropriate adsorption. This was verified with the amounts of Freundlich coefficient n being larger than one which is indicative of physical adsorption. The isotherm data have been drawn using the Langmuir and Freundlich equations and depicted in Figs. 9, 10, and 11. Regression constants are recorded in Table 7. High value of correlation coefficient indicates good contract between the parameters. Values of correlation coefficients show that the Langmuir and Freundlich isotherms are appropriate equations for describing the adsorption equilibrium of DBT on zeolite Y.

HSAB theory indicates that hard acids would rather hard bases and soft acids would rather soft bases. Absolute hardness values of different Lanthanum, sodium, and nickel oxidation states and DBT are listed in Table 8 [39-41].

Ni^{2+} is borderline acid. La^{3+} and Na^{+} are hard acids. DBT is considered as soft base. Therefore, interaction of DBT with Ni^{2+}, La^{3+} and Na^{+} form the following order:

Ni^{2+}-Y > La^{3+}-Y > Na^{+}-Y

Therefore sorbents desulfurization performances decrease as follows:

Ni^{2+}-Y > La^{3+}-Y > Na^{+}-Y

Table 6: Kinetic parameters of adsorption.

pseudo-first order model		
$K_1(min^{-1})$	$q_{e,cal}$ (mg/g)	R^2
0.0522	25.582	0.949
pseudo-second order model		
$K_2(min^{-1})$	$q_{e,cal}$ (mg/g)	R^2
0.00321	15.015	0.9922

Table 6: Kinetic parameters of adsorption.

pseudo-first order model		
$K_1(min^{-1})$	$q_{e,cal}$ (mg/g)	R^2
0.0522	25.582	0.949
pseudo-second order model		
$K_2(min^{-1})$	$q_{e,cal}$ (mg/g)	R^2
0.00321	15.015	0.9922

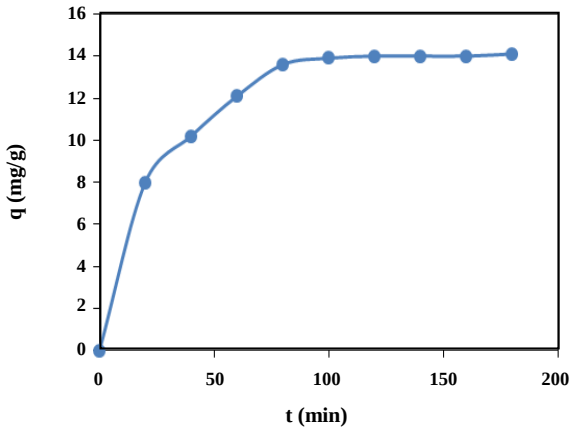

Fig. 6: Effect of contact time on DBT adsorption.

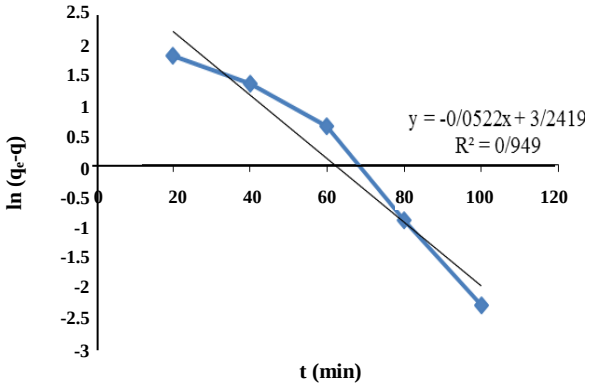

Fig. 7: Results of kinetic analysis: pseudo-first order model.

CONCLUSIONS

In this study, we investigated non-hydrothermal transformation of kaolin into zeolite Na-Y. During preparation of zeolite Y from kaolin, various parameters such as ageing time, crystallization time, and alkali fusion temperature on the model fuel desulfurization were studied. Statistical analysis of experimental data yielded second-order model equation for the one response, sorption capacity. The model was validated by analysis of variance and graphically, and their significance was assessed as well as their very good ability to describe the behavior of the batch adsorption process for desulfurization of model fuel. Optimal DBT adsorbent was synthesized at 550℃ , minimum crystallization time (12h) and maximum aging time (32h). Langmuir and Freundlich isotherm models and approach to adsorption equilibrium curves are discussed. The data was well fitted by both adsorption isotherms. The largest DBT adsorption capacity 32.67 mg DBT/g was calculated for the optimal adsorbent. Kinetic analysis of optimal adsorbent showed that the best fit can be achieved when pseudo-second order model is applied indicating

Table 7: Parameters and constants for the adsorption isotherms of DBT in n-hexane.

Ni-Y	La-Y	Na-Y	Constants	model
0.002537	0.006214	0.002725	b	Langmuir
75.25	66.59	32.67	q_m	
0.9021	0.9928	0.9696	R^2	
0.0951	0.05693	0.0994	R_L	
3.341	5.924	0.9605	k_f	Freundlich
2.513	3.035	2.142	n	
0.9539	0.9881	0.9826	R^2	

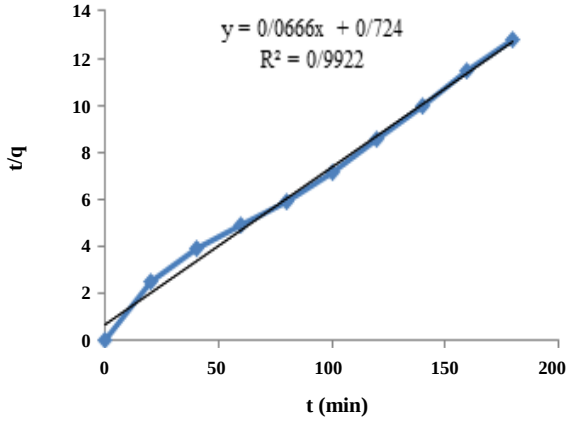

Fig. 8: Results of kinetic analysis: pseudo-second order model.

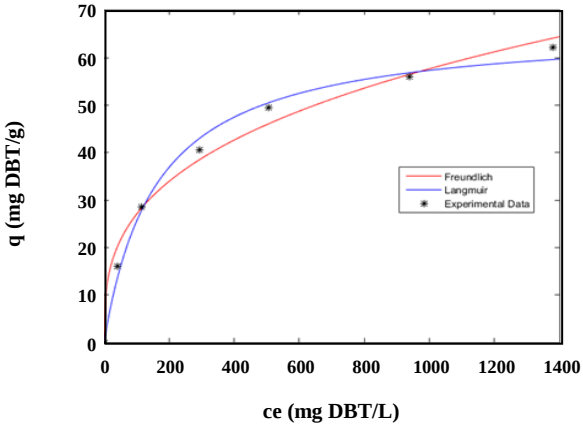

Fig. 10: Isotherms of DBT on La-Y at 25 °C.

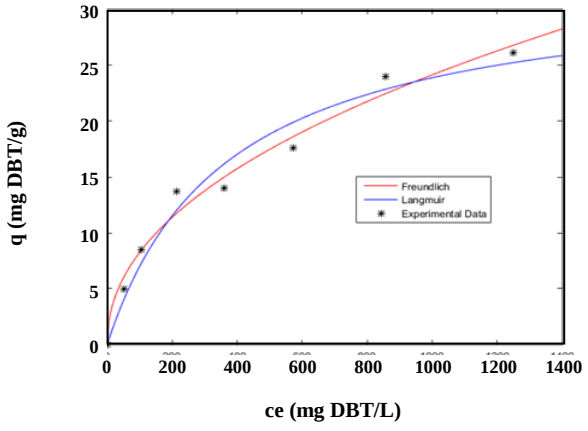

Fig. 9: Isotherms of DBT on Na^I/Y at 25 °C.

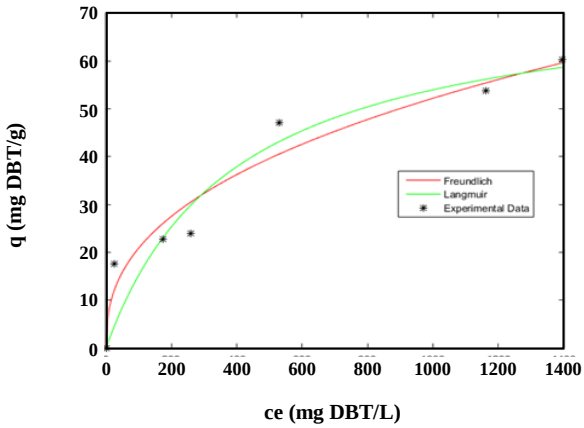

Fig. 11: Isotherms of DBT on Ni-Y at 25 °C.

Table 8: Absolute hardness of compounds based on Pearson classification.

Compound	Absolute Hardness (eV)	Soft/Hard, Acid/Base
Na^{+}	21.1	Hard Acid
Ni^{2+}	8.5	Borderline Acid
La^{3+}	15.4	Hard Acid
DBT	5.267	Soft Base

that adsorption of DBT closely follows second order reaction path. Ni-form and La-form of the optimal zeolite Na-Y are obtained by substitution of sodium ions. Maximum DBT adsorption capacity was observed for Ni–Y (~ 72.25 mg/g) and La–Y (~ 66.59 mg/g) zeolites.

Acknowledgment

The authors are grateful to Stat-Ease, Minneapolis, USA, for the 406 provision of the Design-Expert package.

Nomenclatures

B	Langmuir parameter, L/mg
C_0	Initial concentration, mg DBT/L
C_e	Equilibrium concentration, mg DBT/L
k_1	Pseudo-first order adsorption rate constant, min^{-1}
k_2	Pseudo-second order adsorption rate constant, g/mg.min
m	Mass of adsorbent, g
q	Adsorption capacity at time t, mg DBT/g adsorbent
q_e	Equilibrium adsorption capacity, mg DBT/g adsorbent
q_m	Maximum adsorption capacity, mg DBT/g adsorbent
R_L	Equilibrium parameter
t	time, min
V	Solution volume, L

Received : Jun. 12, 2018 ; Accepted : Oct. 8, 2018

REFERENCES

[1] Kim J.H., Ma X., Zhou A., Song C., Ultra-Deep Desulfurization and Denitrogenation of Diesel Fuel by Selective Adsorption over Three Different Adsorbents: a Study on Adsorptive Selectivity and Mechanism, *Catalysis Today*, **111**: 74-83 (2006).

[2] Muzic M., Sertic-Bionda K., Gomzi Z., Kinetic and Statistical Studies of Adsorptive Desulfurization of Diesel Fuel on Commercial Activated Carbons, *Chemical Engineering & Technology*, **31**: 355-364 (2008).

[3] Ma X., Sun L., Song C., A New Approach to Deep Desulfurization of Gasoline, Diesel Fuel and Jet Fuel by Selective Adsorption for Ultra-Clean Fuels and for Fuel Cell Applications,*Catalysis Today*, **77**: 107-116, (2002).

[4] Song C. E., Lee S.-G., Supported Chiral Catalysts on Inorganic Materials, *Chemical Reviews*, **102**: 3495-3524 (2002).

[5] Selvavathi V., Chidambaram V., Meenakshisundaram A., Sairam B., Sivasankar B., Adsorptive Desulfurization of Diesel on Activated Carbon and Nickel Supported Systems, *Catalysis Today*, **141**: 99-102 (2009).

[6] Salem A.B.S., Naphtha Desulfurization by Adsorption, *Industrial & Engineering Chemistry Research*, **33**: 336-340 (1994).

[7] Mintova S., Olson N.H., Bein T., Electron Microscopy Reveals the Nucleation Mechanism of Zeolite Y from Precursor Colloids, *Angewandte Chemie International Edition*, **38**: 3201-3204 (1999).

[8] Li Q., Creaser D., Sterte J., An Investigation of the Nucleation/Crystallization Kinetics of Nanosized Colloidal Faujasite Zeolites, *Chemistry of Materials*, **14**: 1319-1324 (2002).

[9] Yang R.T., Hernández-Maldonado A.J., Yang F.H., Desulfurization of Transportation Fuels with Zeolites under Ambient Conditions, *Science*, **301**: 79-81 (2003).

[10] Velu S., Ma X., Song C., Selective Adsorption for Removing Sulfur from Jet Fuel over Zeolite-Based Adsorbents, *Industrial & Engineering Chemistry Research*, **42**: 5293-5304 (2003).

[11] Hernández-Maldonado A.J., Yang F.H., Qi G., Yang R.T., Desulfurization of Transportation Fuels by π-Complexation Sorbents: Cu (I)-, Ni (II)-, and Zn (II)-Zeolites, *Applied Catalysis B: Environmental*, **56**: 111-126 (2005).

[12] Hernández-Maldonado A.J., Stamatis S.D., Yang R.T., He A.Z., Cannella W., New Sorbents for Desulfurization of Diesel Fuels via π Complexation: Layered Beds and Regeneration, *Industrial & Engineering Chemistry Research*, **43**: 769-776, (2004).

[13] Htay M., Oo M., Preparation of Zeolite Y Catalyst for Petroleum Cracking, *World Academy of Science, Engineering and Technology*, **48**: 114-120 (2008).

[14] Mallapur V.P., Oubagaranadin J.U.K., Lature S.S., Synthesis of Zeolite from Inorganic Wastes, *IJRET; International Journal of Research in Engineering and Technology*, eISSN: 2319-1163 pISSN: 2321-7308, IC-RICE Conference Issue Nov-2013, Available @ http://www.ijret.org

[15] Kovo A., Hernandez O., Holmes S., Synthesis and Characterization of Zeolite Y and ZSM-5 from Nigerian Ahoko Kaolin Using a Novel, Lower Temperature, Metakaolinization Technique, *Journal of Materials Chemistry*, **19**: 6207-6212 (2009).

[16] Kim Y. C., Jeong J. Y., Hwang J.Y., Kim S.D., Kim W.J., Influencing Factors on Rapid Crystallization of High Silica Nano-Sized Zeolite Y without Organic Template under Atmospheric Pressure, *Journal of Porous Materials*, **16**: 299-306 (2009).

[17] Bosch P., Ortiz L., Schifter I., Synthesis of Faujasite Type Zeolites from Calcined Kaolins, *Industrial & Engineering Chemistry Product Research and Development*, **2**: 401-406 (1983).

[18] Basaldella E., Kikot A., Pereira E., Synthesis of Zeolites from Mechanically Activated Kaolin Clays, *Reactivity of Solids*, **8**: 169-177 (1990).

[19] Wang J.Q., Huang Y.X., Pan Y., Mi J.X., New Hydrothermal Route for the Synthesis of High Purity Nanoparticles of Zeolite Y from Kaolin and Quartz, *Microporous and Mesoporous Materials*, **232**: 77-85 (2016).

[20] Bortolatto L.B., Santa R.A.B., Moreira J.C., Machado D.B., Martins M.A.P., Fiori M.A., Kuhnen N.C., Riella H.G., Synthesis and Characterization of Y Zeolites from Alternative Silicon and Aluminium Sources, *Microporous and Mesoporous Materials*, **248**: 214-221 (2017).

[21] Covarrubias C., García R., Arriagada R., Yánez J., Garland M.T., Cr (III) Exchange on Zeolites Obtained from Kaolin and Natural Mordenite, *Microporous and Mesoporous Materials*, **88**: 220-231 (2006).

[22] Seliem M.K., Komarneni S., Equilibrium and Kinetic Studies for Adsorption of Iron from Aqueous Solution by Synthetic Na-A Zeolites: Statistical Modeling and Optimization, *Microporous and Mesoporous Materials*, **228**: 266-274 (2016).

[23] Wang J.-Q., Huang Y.-X., Pan Y., Mi J.-X., Hydrothermal Synthesis of High Purity Zeolite A from Natural Kaolin Without Calcination, *Microporous and Mesoporous Materials*, **199**: 50-56 (2014).

[24] Abdullahi T., Harun Z., Othman M.H.D., A Review on Sustainable Synthesis of Zeolite from Kaolinite Resources via Hydrothermal Process, *Advanced Powder Technology*, **28**: 1827-1840**,** *(*2017).

[25] Ma Y., Yan C., Alshameri A., Qiu X., Zhou C., Synthesis and Characterization of 13X Zeolite from Low-Grade Natural Kaolin, *Advanced Powder Technology*, **25**: 495-499 (2014).

[26] Song C., An Overview of New Approaches to Deep Desulfurization for Ultra-Clean Gasoline, Diesel Fuel and Jet Fuel, *Catalysis Today*, **86**: 211-263, (2003).

[27] Song C., Ma X., New Design Approaches to Ultra-Clean Diesel Fuels by Deep Desulfurization and Deep Dearomatization, *Applied Catalysis B: Environmental*, **41**: 207-238 (2003).

[28] Oyinade A., Kovo A.S., Hill P., Synthesis, Characterization and Ion Exchange Isotherm of Zeolite Y Using Box–Behnken Design, *Advanced Powder Technology*, **27**: 750-755 (2016).

[29] Bakhtiari G., Bazmi M., Abdouss M., Royaee S.J., Adsorption and Desorption of Sulfur Compounds by Improved Nano Adsorbent: Optimization Using Response Surface Methodology, *Iranian Journal of Chemistry and Chemical Engineering (IJCCE)*, **36**: 69-79 (2017).

[30] Jiang M., Ng F.T., Adsorption of benzothiophene on Y Zeolites Investigated by Infrared Spectroscopy and Flow Calorimetry, *Catalysis Today*, **116**: 530-536 (2006).

[31] Yao Z.-Y., Qi J.-H., Wang L.-H., Equilibrium, Kinetic and Thermodynamic Studies on the Biosorption of Cu (II) onto Chestnut Shell, *Journal of Hazardous Materials*, **174**: 137-143 (2010).

[32] Kumar S., Zafar M., Prajapati J.K., Kumar S., Kannepalli S., Modeling Studies on Simultaneous Adsorption of Phenol and Resorcinol onto Granular Activated Carbon from Simulated Aqueous Solution, *Journal of Hazardous Materials*, **185**: 287-294 (2011).

[33] Jha V.K., Nagae M., Matsuda M., Miyake M., Zeolite Formation from Coal Fly Ash and Heavy Metal Ion Removal Characteristics of Thus-Obtained Zeolite X in Multi-metal Systems, *Journal of Environmental Management*, **90**: 2507-2514 (2009).

[34] Samiee Beyragh A., Varsei M., Meshkini M., Khodadadi Darban A., Gholami E., Kinetic and Adsorption Isotherms Study of Cyanide Removal from Gold Processing Wastewater Using Natural and Impregnated Zeolites, *Iranian Journal of Chemistry and Chemical Engineering (IJCCE)*, **37**(2):139-149 (2018).

[35] Araissi M., Elaloui E., Moussaoui Y., The removal of Cadmium, Cobalt and Nickel by Adsorption with Na-Y Zeolite, *Iranian Journal of Chemistry and Chemical Engineering (IJCCE)*, (2018). [in Press]

[36] Sang S., Liu Z., Tian P., Liu Z., Qu L., Zhang Y., Synthesis of Small Crystals Zeolite NaY, *Materials Letters*, **60**: 1131-1133 (2006).

[37] Nibou D., Mekatel H., Amokrane S., Barkat M., Trari M., Adsorption of Zn^{2+} Ions onto NaA and NaX Zeolites: Kinetic, Equilibrium and Thermodynamic Studies, *Journal of Hazardous Materials*, **173**: 637-646 (2010).

[38] Kalhor M., Seyedzade Z., Ni@ Zeolite-Y Nano-Porous: Preparation and Application as a High Efficient Catalyst for Facile Synthesis of Quinoxaline, Pyridopyrazine and Indoloquinoxaline Derivatives, *Iranian Journal of Chemistry and Chemical Engineering (IJCCE)*, **38**(1): 27-41 (2019).

[39] Parr R. G., Pearson R.G., Absolute Hardness: Companion Parameter to Absolute Electronegativity, *Journal of the American Chemical Society*, **105**: 7512-7516 (1983).

[40] Pearson R.G., Hard and Soft Acids and Bases, *Journal of the American Chemical Society*, **85**: 3533-3539 (1963).

[41] Xiao J., Li Z., Liu B., Xia Q., Yu M., Adsorption of Benzothiophene and Dibenzothiophene on Ion-Impregnated Activated Carbons and Ion-Exchanged Y Zeolites, *Energy & Fuels*, **22**: 3858-3863 (2008).